

Synthesis and characterization of polyaniline Zr(IV) molybdophosphate for the adsorption of phenol from aqueous solution

Meraj Alam Khan · Mohammed Kashif Uddin ·
Rani Bushra · Anees Ahmad · Syed Ashfaq Nabi

Received: 7 March 2014 / Accepted: 30 June 2014 / Published online: 24 July 2014
© Akadémiai Kiadó, Budapest, Hungary 2014

Abstract In the present investigation, a composite cation exchange material has been synthesized by the sol–gel method and used as an adsorbent for the removal of phenol from aqueous solutions. Scanning electron microscope, Fourier transform infrared spectroscopy, X-ray diffraction and transmission electron microscopy studies were performed to characterize the polyaniline Zr(IV) molybdophosphate (PZMP) particles. The average size of the PZMP was in the nano-range. Batch adsorption studies were carried out to study the effect of various parameters like effect of pH, initial concentration, contact time and temperature. Increase in the initial phenol concentration with time could effectively increase the phenol adsorption capacity. Adsorption data of phenol agreed well with Langmuir, Freundlich, Temkin and Dubinin–Redushkeuich (D–R) isotherms at different temperatures. The maximum phenol adsorption capacity was obtained as 25.144 mg/g for 50 mg/L initial phenol concentrations. Thermodynamic parameters showed that adsorption of phenol were endothermic, spontaneous and thermodynamically favorable. The kinetic data followed pseudo-second order kinetic model.

Keywords Composite · Adsorption · Isotherms model · Kinetics · Thermodynamics

M. A. Khan · R. Bushra · A. Ahmad (✉) · S. A. Nabi
Department of Chemistry, Aligarh Muslim University, Aligarh, India
e-mail: bushra.rani786@gmail.com

M. K. Uddin
Basic Engineering Sciences Department, College of Engineering, Majmaah University, Majmaah,
Kingdom of Saudi Arabia

Introduction

The spread of a wide range of contaminants in aqueous solution has become a major environmental problem worldwide. Various organic and inorganic compounds are present in the wastewater streams of many industrial processes. Rapid development of industrialization such as dyeing, printing, plastic, mining and metallurgical engineering, electroplating, nuclear power plants, semiconductor and battery manufacturing processes are some of the industries that are generating various types of pollutants in the wastewater effluents. All of these contaminants are harmful to human beings and ecological environment human health due to its higher toxicity which can lead to severe diseases and problems. Phenols are generally considered as one of the important organic pollutants discharged into the environment because they are harmful to organisms at low concentrations [1, 2]. Therefore, Environmental Protection Agency regulations call for lowering phenol content in wastewater to less than 1 mg/L [3]. It is thus essential to control the discharge of phenol into water bodies. Many novel adsorbents have recently been used for the removal of toxic phenol [4–10]. Various techniques have been employed for the removal of toxic pollutants from water solution but the adsorption technique has numerous advantages such as high speed, versatility, effectiveness, regeneration for multiple uses and high selectivity [11]. This technique is a physical separation process used in wastewater treatment to remove toxic organic pollutants and heavy metals especially when present at low concentrations.

In recent years, polymeric–inorganic composites have attracted great interest, both in industry and in academy, because they often exhibit remarkable improvements in material properties when compared with conventional polymers. The development of inorganic–organic hybrid materials is especially trendy in the last decade. Within the vast collection of inorganic–organic hybrid materials, nanocomposites are an emerging group that received a great deal of attention not only because of their potential in industrial applications but also from their fundamental point of view [12, 13]. Efforts have been made to improve the chemical, thermal and mechanical stabilities of ion exchangers and to make them highly selective for certain metal ions. A number of such materials were prepared in the laboratory by incorporating polyaniline, polypyrrole, polyanisidine and poly-*o*-toluidine into the precipitate of elements of III, IV, V and VI group of the periodic table [14]. Few such excellent ion exchange materials have been developed and successfully being used in chromatographic techniques [15, 16]. Electrical conductivity (in the semiconducting region) along with the chromatographic behavior of these composites attracted researchers to investigate more possible applications in the field of environmental science engineering [17–19].

In the present study, polyaniline Zr(IV) molybdophosphate (PZMP) has been synthesized to check its adsorptive potential towards phenol. The objective of this work was to investigate the effect of pH, time, concentration and temperature to determine the various isotherms, kinetics, thermodynamic and equilibrium properties of phenol adsorption. Several characterization techniques were also used in order to determine the applicability of this ion exchange material in the adsorption studies. PZMP has not yet been tested for the adsorption of phenol from aqueous

solution and thus its excellent adsorption capacity and technological applications give the novelty to this paper.

Experimental

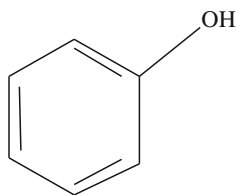
Reagents and instruments

The main reagents for the synthesis were aniline, potassium persulfate, zirconium oxychloride, sodium molybdate, orthophosphoric acid which is procured from E-Merck (India). All other reagents and chemicals were of analytical grade (AR grade). Solutions of zirconium oxychloride (0.25 M), orthophosphoric acid (0.25 M), sodium molybdate (0.25 M) were all prepared in demineralized water (DMW) while a 10 % solution (v/v) of aniline and 0.10 M potassium persulfate were prepared in a 1 M HCl solution. A stock solution of phenol was prepared (1,000 mg/L) in ethanol. Solutions were then diluted to the desired concentration in demineralized water for further study.

A LabIndia UV-3200 double beam spectrophotometer with 10 mm matched quartz cells was used for spectrophotometric determination. The infrared (IR) spectra was recorded on a Fourier transform infrared spectroscopy (FTIR) Spectrometer [Perkin Elmer (1730, USA)] using KBr disc method. An X'Pert PRO analytical diffractometer (PW-3040/60 Netherlands with CuK_α radiation $\lambda = 1.5418 \text{ \AA}$) was used for X-ray diffraction (XRD) measurement. The scanning electron microscopy instrument (SEM; LEO, 435 VF) was used for SEM images of the material at different magnifications. Transmission electron microscopy (TEM) analysis was carried out on a Jeol H-7500.

Adsorbate

Phenol has the following chemical structure and its molar mass is 94.111. The cross sectional area (nm^2/mol) of phenol is 0.42 nm^2 [20] while its solubility in water (g/L) at $20 \text{ }^\circ\text{C}$ is 82 [21].



Synthesis of polyaniline

The polymerization of aniline was initiated by adding potassium persulfate into 10 % solution of aniline in 1:1 ratio while maintaining the temperature below $10 \text{ }^\circ\text{C}$ under constant stirring for 1 h [20], a dark green gel of polyaniline was obtained.

Synthesis of inorganic precipitate Zr(IV) molybdophosphate

Inorganic precipitate of Zr(IV) molybdophosphate was prepared by adding a aqueous solution of zirconium(IV) oxychloride into a solution of molybdophosphate in different molarities at the flow rate of 2.0 mL/min. Continuous stirring was done during mixing using a magnetic stirrer and in result yellow gel type slurry was obtained. The resulting yellow precipitate was then allowed to stand for 24 h in the mother liquor for digestion.

Synthesis of polyaniline Zr(IV) molybdophosphate

The polyaniline Zr(IV) molybdophosphate composite material was prepared by the mixing of inorganic precipitate and polyaniline gel (in 1:1 volume ratio) with continuous stirring for 1 h at 25 ± 2 °C. The resultant dark green gel was kept for 24 h at room temperature for digestion. The supernatant liquid was decanted and the gel was filtered under suction. The excess acid was removed by washing with demineralized water and then the material was dried in an oven at 50 ± 2 °C. The dried material was grounded into small granules, sieved and converted into H^+ form by treating with 1.0 M nitric acid solution for 24 h with occasional shaking intermittently replacing the supernatant liquid with fresh acid. The excess acid was removed after several washings with DMW and finally dried at 50 ± 2 °C in an oven. By applying the above chemical route, a number of samples of polyaniline Zr(IV) molybdophosphate composite were synthesized under different conditions of mixing volume ratios of reactants. On the basis of good ion exchange capacity, percentage yield, sample Z-8 was selected for detailed studies (Table 1).

Adsorption studies

Adsorption studies were carried out by batch process. 0.25 g adsorbent was placed in a conical flask in which 25 mL solution of phenol of desired concentration was added and the mixture was shaken in temperature controlled shaker incubator and then filtered using Whatman filter 41 and final concentration of pollutant was determined in the filtrate by UV spectrophotometer at wavelength of 270 nm.

Characterizations of the adsorbent

X-Ray diffraction was used for the identification of crystal structures. SEM was used to identify the surface quality and morphology of the adsorbent before and after adsorption. In order to identify the binding groups present before and after adsorption on the adsorbent surface and their involvement in adsorption process, FTIR was recorded. Transmission electron microscopy images were also recorded to determine the average particle size of the adsorbent.

Table 1 Conditions for the synthesis of polyamine Zr(IV) molybdophosphate cation exchanger

S.No	A	B	C	D	Mixing ratio v/v/v (A:B:C)	E:D v/v	pH	Appearance of bead	IEC for Na ⁺ ions	Yield (g)
Z-1	0.25	0.25	0.25	1:1:1	0.50	Yellow	0.76	3.17
Z-2	0.25	0.25	0.25	1:1:1	1.0	Yellow	0.47	7.53
Z-3	0.25	0.25	0.25	1:1:1	1.5	Yellow	0.45	7.34
Z-4	0.25	0.25	0.25	1:1:1	0.75	Yellow	0.32	7.67
Z-5	0.25	0.25	0.25	1:1:2	0.75	Yellow	1.22	8.51
Z-6	0.25	0.25	0.25	1:2:1	0.75	Yellow	0.29	6.24
Z-7	0.25	0.25	0.25	10	1:1	0.75	Green	1.1	4.3
Z-8	0.25	0.25	0.25	10	1:2	0.75	Green	1.3	5.3
Z-9	0.25	0.25	0.25	10	1:2	1.0	Green	0.99	4.2
Z-10	0.25	0.25	0.25	10	1:2	1.5	Green	0.67	3.4

A zirconium (IV) oxychloride (Mol/L), B sodium molybdate (Mol/L), C Orthophosphoric acid (Mol/L), D polyamine (stock solution of 10 % aniline), IEC Ion exchange Capacity (meq/g), E:D [A:B:C] :D

Effect of temperature

The effect of temperature on the adsorption of phenol was studied by varying the adsorbent doses from 0.4 to 1.0 g at fixed volume (25 mL) of the phenol solution with initial concentration of 25 mg/L in conical flasks. These flasks were kept in a temperature controlled water bath shaker at different temperatures (30–50 °C) for 4 h at 150 rpm to reach the equilibrium and then filtered. The final concentration of the compound in the filtrate from each flask was then determined as described earlier.

Effect of pH

The experiment was performed by taking 0.25 g of PZMP into twelve (250 ml) conical flasks. 25 ml of 25 mgL⁻¹ solutions of phenol were added into it. The pH value of these suspensions was adjusted to 2.0, 4.0, 6.0, 8.0, 10.0 and 12.0 by adding a solution of conc. HCl or NaOH and after equilibrium, the final pH of phenol was determined using pH meter (ELICO-Li, India).

Effect of contact time and initial concentration

Effect of time on the adsorption of phenol was determined separately by analyzing the residual pollutant in the liquid after contact period from 5 to 180 min. Experiments were performed using batch process at room temperature. 0.25 g of adsorbent was added to 25 mL solution of various initial concentrations of phenol (10–100 mg/L). Samples were withdrawn from conical flasks after specified time interval and analyzed for residual phenol content.

Results and discussion

Characterizations of the adsorbent

The functional groups or the binding sites were identified by FTIR spectra of native and treated adsorbent with a view to understand the surface binding mechanism. Figs. 1a and 1b show the FTIR spectra of polyaniline Zr(IV) molybdophosphate before and after phenol adsorption and represented the comparison of FTIR spectrum of native and phenol treated PZMP. The FTIR spectrum of the composite cation exchanger (Fig. 1a) indicates the presence of external water molecules in addition to the OH groups and metal oxides present internally in the material. The peak at 1,508 cm⁻¹ is characteristic of the deformation of the free water molecules [22]. The broad peak in the region at 1,064 and 1,060 cm⁻¹ represents the presence of ionic phosphate groups [23] in the material. The characteristic peaks at around 1,481 and 1,569 cm⁻¹ are attributed to the C=N stretching mode of quinoid (Q) rings and C=C stretching mode of benzenoid (B) rings, respectively, as these peaks correspond to the most of the characteristic peaks for PANI as described in literature [24, 25]. The peaks at 1,397 cm⁻¹ may be due to deformation vibration of metal hydroxyl group. A sharp peak at 799 cm⁻¹ is due to the presence of

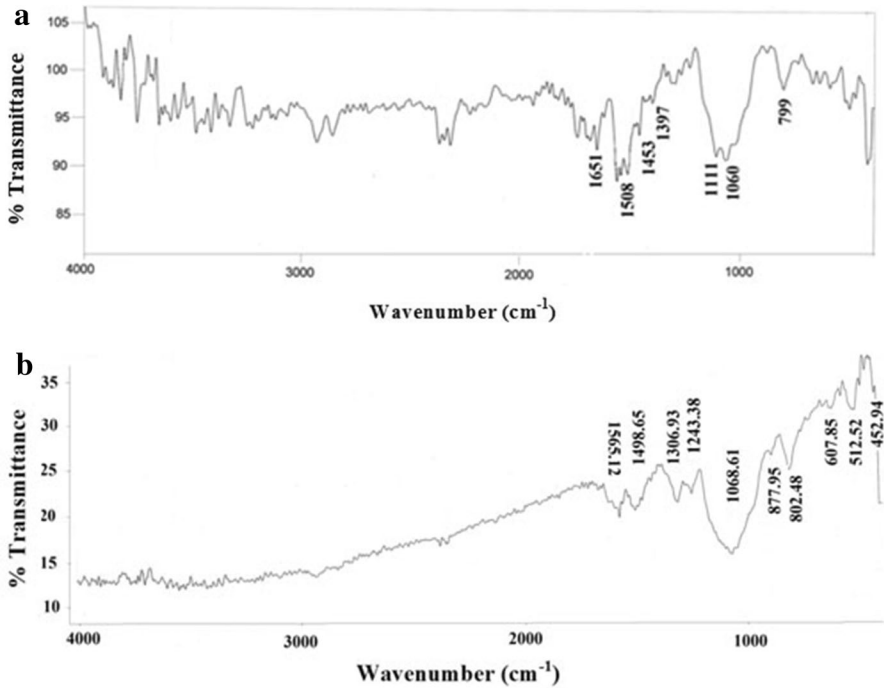


Fig. 1 **a** FTIR of polyaniline Zr(IV) molybdophosphate, **b** FTIR of phenol treated polyaniline Zr(IV) molybdophosphate

molybdate group [26]. An assembly of peaks in the region 500–650 cm^{-1} was due to the metal–oxygen stretching vibrations. However, there were some new peaks were observed in treated adsorbent showing that the adsorption process takes place at the surface of adsorbent. There were shifts in the wave number of peaks associated with the treated adsorbent (Fig. 1b). These shifts in band indicate that there was a high potential for binding process. A clear shift from 1,508 to 1,565.12 cm^{-1} after phenol treatment was due to C = C stretching. The shift from 1,397 to 1,306.93 cm^{-1} assigned to N–O stretch. The peaks at 1068.61 cm^{-1} in treated adsorbent assigned to C–O stretching vibration. The peaks from 600–400 cm^{-1} showed strong adsorption due to C≡C–H bend.

Scanning electron microscopy

The SEM analysis gives a sufficient general summary of the surface morphology of the adsorbent. The SEM micrographs of native and phenol treated PZMP are shown in Figs. 2a, b, c and d. The morphology of the surface is slightly changed after phenol adsorption (Figs. 2c and d). Adsorbed phenol on the surface of the PZMP can be seen clearly in the form of white patches (Figs. 2c and d). As compared to native (Figs. 2a and b), the surface of adsorbed phenol PZMP is more irregular and porous, which indicates that the surface area and pore volume increased. The distinct morphology is due to the aggregates of phenol deposition, which may

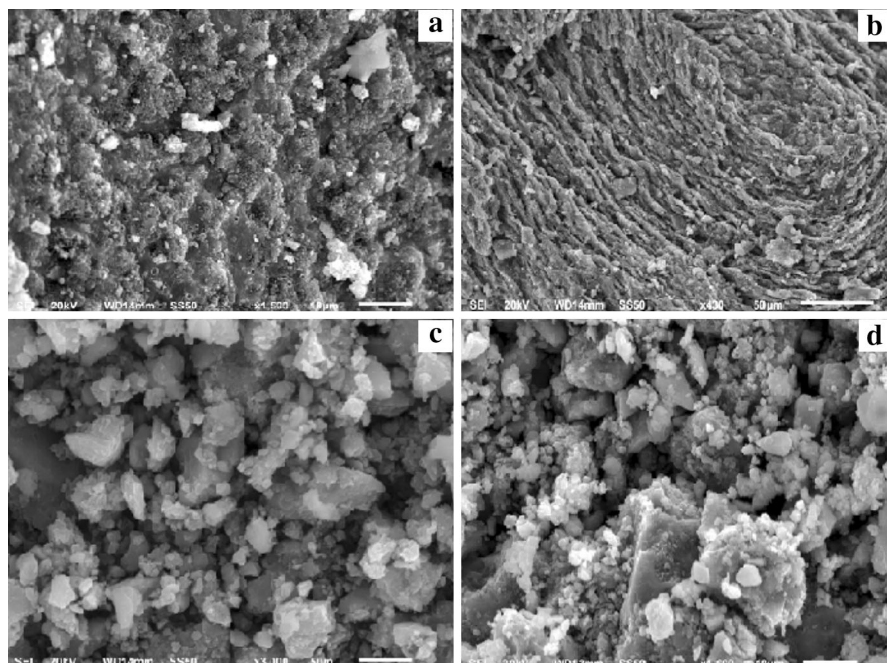


Fig. 2 a, b Scanning electron microscopy (SEM) analysis of polyaniline Zr(IV) molybdophosphate c, d phenol treated polyaniline Zr(IV) molybdophosphate

briefly indicate that the pores were prominent on the surface of adsorbent before adsorption (Figs. 2a and b) and after the adsorption of phenol, the pores were filled showing adherence of phenol on the surface (Figs. 2c and d) in the form of white patches. These large pores and increased surface area are important factors to enhance intake of phenol.

X-Ray diffraction and transmission electron microscopy

The X-ray diffractogram in Fig. 3 shows some prominent peaks together with a number of low intensity peaks, which suggests the semi-crystalline nature of the composite material. TEM studies revealed that composite cation exchange material (Fig. 4) has the particles size in the range of 50–100 nm and thus the particle size was found to be in nano-range.

Effect of time and initial concentration

The effect of contact time and concentration on the adsorption of phenol is shown in Fig. 5. It has been found that the adsorption was concentration dependent and increased with increase in initial concentrations. The equilibrium adsorption capacities at 10, 30, 60 and 100 mg/L initial phenol concentrations were found to be 1.49, 2.84, 5.80 and 9.6 mg/g. The initial adsorption rate was high for phenol (30 min) and then slowed down while approaching towards equilibrium. The initial

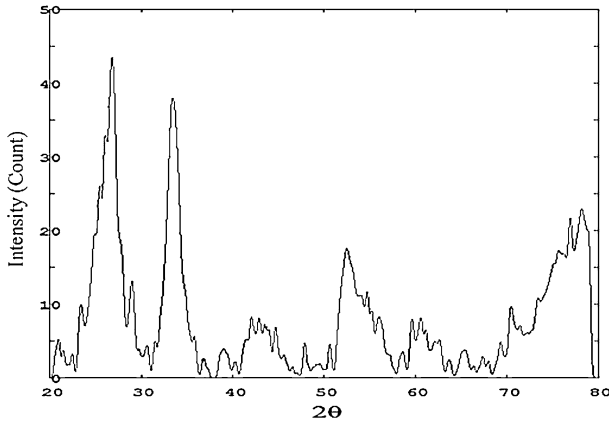


Fig. 3 X-ray diffraction pattern of polyaniline Zr(IV) molybdophosphate

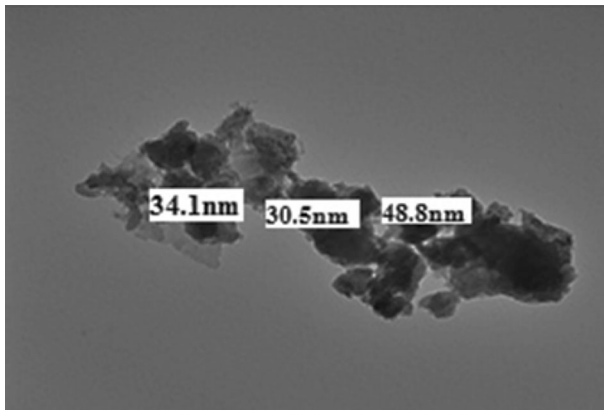


Fig. 4 TEM image of polyaniline Zr(IV) molybdophosphate

adsorption rate of phenol increased with increase in concentration which might be due to increased driving force and a large number of vacant surface sites was available for adsorption during the initial stage. With the increase of time, the remaining vacant surface sites were difficult to be occupied due to repulsive forces between the solute molecules on the solid and bulk phases while after saturation of adsorption sites, the adsorption of phenol proceeded towards equilibrium through pore diffusion (a slow process). The equilibrium time for the adsorption of phenol was found to be 120 min at 10, 30, 60 and 100 mg/L initial phenol concentrations.

Effect of pH

The effect of pH is the most critical parameter which affects the adsorption process and this may be because the charge of both adsorbate and adsorbent often

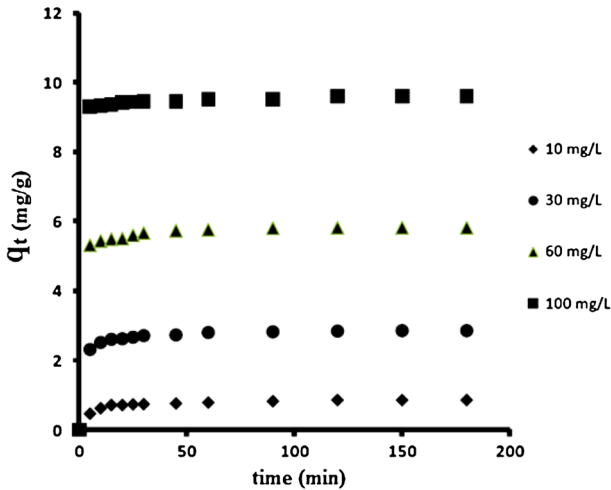


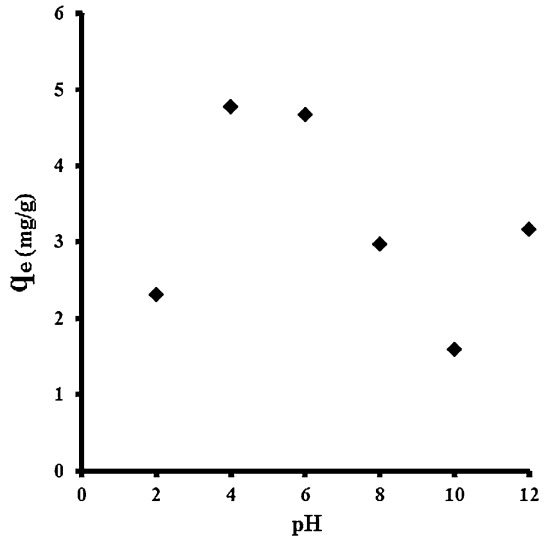
Fig. 5 Effect of contact time on the sorption of phenol on the nanocomposite material at different phenol concentrations

depends on the pH of the solution. The adsorption of phenol on PZMP was studied in the pH range between 2 to 12. Fig. 6 shows the effect of pH on the phenol adsorption using PZMP under the given conditions. The adsorption capacity decreases with an increase in pH (up to pH 8) and then increased slightly with a further increase in pH (up to pH 12). The optimal adsorption capacity of phenol onto PZMP takes place in the pH region 4–6. A sharp decrease in adsorption capacity was observed up to pH 6.0, while with further increase in pH, a significant decline in adsorption may be attributed to formation of the phenolate anions. At pH 2, the surface of the adsorbent would be protonated and these led to donor–acceptor interactions between the aromatic rings of the phenol [27], while at high pH values (pH 10–12), the phenol would be ionized in solution which led to the increase in ionic strength [28] results in the further increase of adsorption capacity [28].

Adsorption isotherms

In order to optimize the design of the adsorption system for the removal of phenol from aqueous solution, it is important to explain the relationship between adsorbed metal ion per unit weight of adsorbent (q_e) and residual concentration of metal ions in solution (C_e) at equilibrium. Experimental data for the adsorption were fitted in the Langmuir, Freundlich, and Temkin models at different temperatures and results are reported in Fig. 7 and Table 2. The fitting procedure was performed by using R-software version 2.10.1 (2009-12-14). In order to evaluate the fitness of the data, determination coefficient (R^2), residual error analysis (RSE) were evaluated between experimental and calculated data from each model.

Fig. 6 Effect of pH on the sorption of phenol on nanocomposite polyaniline Zr(IV) molybdophosphate



According to the Langmuir model [29], the adsorption occurs on a homogenous surface forming monolayer of adsorbate with constant heat of adsorption for all sites without interaction between adsorbed molecules [30]. The linear form of the Langmuir model may be given as

$$\frac{1}{q_e} = \frac{1}{q_m} \times \frac{1}{b} \times \frac{1}{C_e} + \frac{1}{q_m} \tag{1}$$

where C_e is the equilibrium concentration of metal ions in the solution (mg/L), q_e is the amount of metal ion adsorbed per unit weight of adsorbent (mg/g), q_m is the amount of metal ion required to form monolayer (mg/g) or maximum monolayer adsorption capacity and b is a constant related to energy of adsorption (L/mg) which represents enthalpy of adsorption and should vary with temperature. In the case of phenol adsorption, plots of $1/q_e$ versus $1/C_e$ at 30, 40 and 50 °C gave straight lines and the values of b and q_m were calculated from the slope and intercept of the plots shown in Fig. 7a. The values of q_m and b increase with increasing temperature, indicating a higher heat of adsorption with increasing temperature and the endothermic nature of the adsorption. The data obtained from this model were fitted well at all temperatures as shown by high determination coefficient (R^2), least p value and RSE values (Table 2). The maximum monolayer adsorption capacity of PZMP for phenol was compared with other adsorbents, reported earlier (Table 3). It has been found that the adsorption capacity of PZMP is higher than those reported in the literature [8–10, 31].

The Freundlich isotherm model [32] can be applied to multilayer adsorption with non-uniform distribution of adsorption heat and affinities over the heterogeneous surface [33]. The linear form of the Freundlich model can be represented as

$$\log q_e = \log K_f + \frac{1}{n} \log C_e \tag{2}$$

where C_e is the equilibrium concentration in mg/L and q_e shows that the adsorption seems to follow the Freundlich isotherm model as well as Langmuir isotherm, K_f is

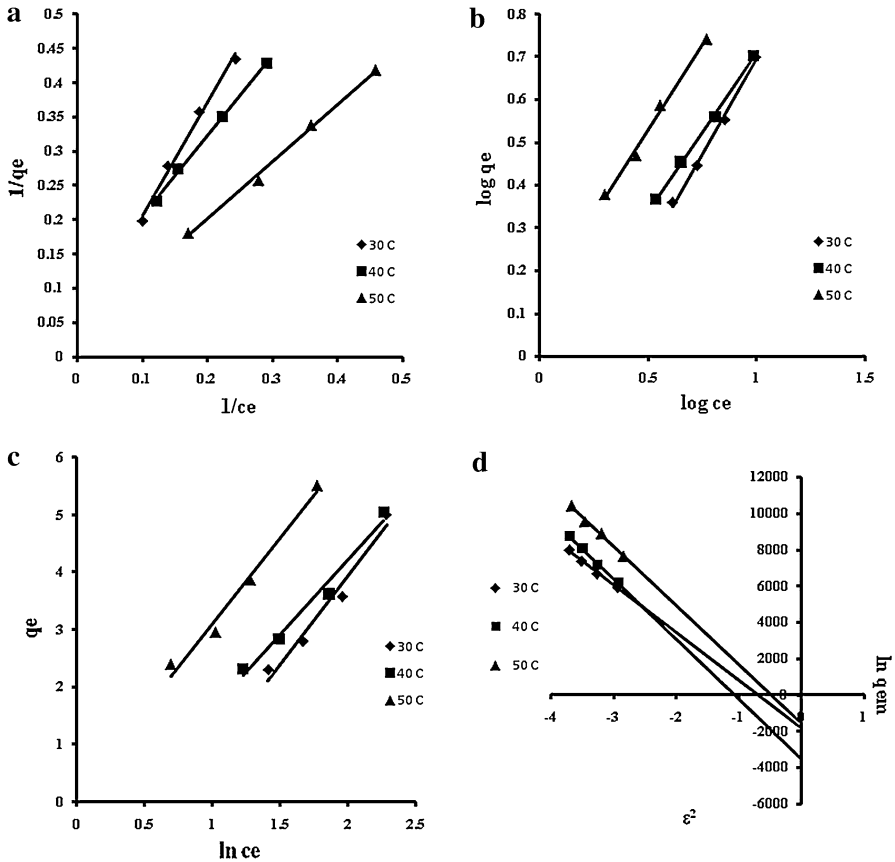


Fig. 7 Isotherms for the adsorption of phenol on polyaniline Zr(IV) molybdophosphate. **a** Langmuir plot **b** Freundlich plot **c** Temkin plot **d** D–R isotherm plot

the Freundlich constant which indicates the relative adsorption capacity of the adsorbent related to bonding energy and n is the heterogeneity factor representing the deviation from the linearity of adsorption and is also known as the Freundlich coefficient. Plots of $\log q_e$ versus $\log C_e$ for the adsorption of phenol generated straight lines at 30, 40 and 50 °C and was well obeyed at all temperatures as shown in Fig. 7b. The values of n and K_f were calculated from the slope and intercept of these plots. The values of Freundlich constant increased with increase in temperature, suggesting that adsorption of phenol was endothermic. The value of n , are higher than 1 indicates that adsorption capacity was favored over the entire range of studied data [34] (Table 2).

The Temkin isotherm [35] assumes that the decrease in the heat of adsorption is linear rather than logarithmic, as implied in the Freundlich isotherm [36]. The linear form of Temkin equation can be represented as

Table 2 Adsorption isotherm parameters for the adsorption of phenol onto PZMP

Isotherms	Parameters	30 °C	40 °C	50 °C
Langmuir	B (L/mg)	0.024	0.065	0.825
	qm (mg/g)	25.144	12.581	1.658
	R ²	0.993	0.995	0.989
	RSE	0.010	0.007	0.013
	p value	<0.050	<0.050	<0.050
Freundlich	K (mg/g) (L/mg) ^{1/n}	0.638	0.937	1.364
	n (g/L)	1.212	1.354	1.264
	R ²	0.995	0.998	0.993
	RSE	0.012	0.007	0.015
	p value	<0.050	<0.050	<0.050
Temkin	A (L/mg)	0.187	0.416	1.113
	B (J/mol)	868.731	1001.455	847.226
	R ²	0.964	0.979	0.981
	RSE	0.261	0.210	0.229
	p value	<0.050	<0.050	<0.050
D–R	qm (mol/g)	0.132	0.112	0.144
	K (mol ² J ²)	2.382 × 10 ⁻⁸	2.021 × 10 ⁻⁸	1.934 × 10 ⁻⁸
	E (kJ/mol)	14.744	15.811	16.322
	R ²	0.985	0.991	0.990
	RSE	0.043	0.037	0.049
	p value	<0.050	<0.050	<0.050

Table 3 Comparison of the adsorption capacities for phenol onto various adsorbents

Adsorbent	Adsorption capacity (mg/g)	Reference
N-doped carbon nanotube	9.411	[8]
Hydroxyapatite nanopowder	10.33	[9]
CMCD-LDH	0.824	[10]
Amphiphilic hybrid material	18.18	[31]
PZMP	25.144	Present study

$$q_e = \left(\frac{RT}{b}\right) \times \ln A + \left(\frac{RT}{b}\right) \times \ln C_e \tag{3}$$

Here, (RT/b) = B, R is universal gas constant, T is absolute temperature and b is another constant. A (g/L) and B (J/mol) are Temkin constants related to adsorption potential and heat of adsorption. The values of A and B can be calculated from the slope and intercept of the plot of q_e versus ln C_e (Fig. 7c). The data obtained from Temkin model (Table 2) for the adsorption of phenol indicates that this model was fitted well as shown by high determination coefficient (R² = 0.961–0.981), least p-value and RSE values.

The Dubinin–Redushkeuich (D–R) isotherm [37] does not assume a homogenous surface or a constant sorption potential [38]. The Dubinin–Radushkevich model was chosen to estimate the characteristic porosity and the apparent free energy of adsorption. The linear forms of this equation are represented as

$$\ln q_e = \ln q_m - \beta \varepsilon^2 \quad (4)$$

$$\varepsilon = RT \ln \left(1 + \frac{1}{C_e} \right) \quad (5)$$

$$E = \frac{1}{\sqrt{(-2\beta)}} \quad (6)$$

Here, ε is the Polanyi potential, q_m is the monolayer capacity (mol/g) and C_e is the equilibrium concentration (mol/L). The Polanyi potential (ε) and mean free energy of adsorption (E , kJ/mol) can be calculated from the equations. β is the D–R model constant (mol²/kJ) or the porosity factor which can be obtained from the slope of the plot of $\ln q_e$ versus ε^2 (Fig. 7d). The values of E lie between 8 and 16 kJ/mol, which depict that the adsorption process follows the chemical ion exchange and if $E < 8$ kJ/mol, the adsorption process is of a physical nature [39]. In this study, the positive value of energy (E) of adsorption confirms that the adsorption process was endothermic. The higher values of the mean free adsorption energy determined using the D–R equation (Table 2) reveal that the adsorption of phenol on PZMP involved physical adsorption due to the Van der Waals forces.

It can be concluded that the above models are well fitted for phenol adsorption on PZMP at different temperatures. The p value for all the models at 30, 40 and 50 °C were less than 0.05 ($p < 0.05$). Table 2 describes the isotherm data of phenol obtained from the Langmuir, Freundlich, Temkin and D–R models at different temperatures.

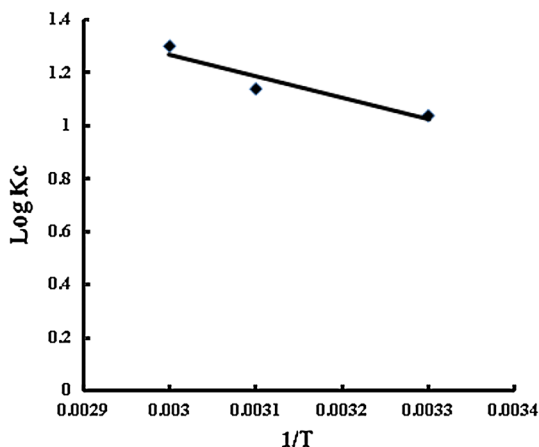
Thermodynamic study

The effect of temperature on the adsorption of phenol was studied in the temperature range from 30–50 °C. Thermodynamic parameters such as standard free energy change (ΔG°), standard enthalpy change (ΔH°) and standard entropy change (ΔS°) were estimated using the following relations [40]

$$K_c = \frac{C_{Ad}}{C_e} \quad (7)$$

Here, K_c is the distribution constant, C_{Ad} and C_e are equilibrium concentrations of target pollutant on the adsorbent and in the solution, respectively. According to the IUPAC recommendations [41], the distribution constant is defined as the ratio of the concentration of a substance in a single definite form in the extract to its concentration in the same form in the other phase at equilibrium. The Gibbs energy change (ΔG°) indicates the degree of spontaneity of an adsorption process, and a

Fig. 8 Van't Hoff plot for the adsorption of phenol onto polyaniline Zr(IV) molybdophosphate



higher negative value reflects a more energetically favorable adsorption. According to thermodynamic laws, ΔG° of adsorption is calculated as follows

$$\Delta G^\circ = -RT \log K_c \tag{8}$$

Here, ΔG° is the Gibbs free energy, K_c is the thermodynamic equilibrium constant without units, T is the temperature in Kelvin and R is the gas constant. The values of ΔH° and ΔS° were calculated from the following Van't Hoff equation

$$\log K_c = -\frac{\Delta H^\circ}{RT} + \frac{\Delta S^\circ}{R} \tag{9}$$

ΔH° and ΔS° were calculated from the slope and intercept of the plot of $\log K_c$ versus $1/T$ (Fig. 8). The values of the thermodynamic parameters are reported in Table 4. These thermodynamic parameter estimates can offer insight into the type and mechanism of an adsorption process (reported in Table 4). Values of free energy change (ΔG°) were negative confirming that adsorption of phenol was spontaneous and thermodynamically favorable since ΔG° of phenol adsorption becomes more negative with increase in temperature, it also reflects whether physisorption (ΔG° values range from -20 to 0 kJ/mol) or chemisorption (ΔG° values range from -80 to 400 kJ/mol). Adsorption of phenol was endothermic as confirmed by the positive ΔH° value (Table 4). A positive value of ΔS° for the adsorption of phenol (Table 4) in the temperature range 30 – 50 °C suggests an increase in randomness at the adsorbent-adsorbate interface during adsorption since adsorption of phenol dislodge some water molecules from the surface of the adsorbent that resulted in increased randomness.

Adsorption kinetics

In order to understand mechanism of the adsorption process and to analyze the adsorption rate, the kinetic data were modelled to test experimental data using the

Table 4 Thermodynamic parameters at different temperatures for the adsorption of phenol

Temperature (°C)	log Kc	$\Delta\hat{G}$ (kJ/mol)	$\Delta\hat{H}$ (kJ/mol)	$\Delta\hat{S}$ (kJ/mol/K)	R ²
30	1.04	−6.02	42.54	71.02	0.90
40	1.14	−6.82			
50	1.30	−8.02			

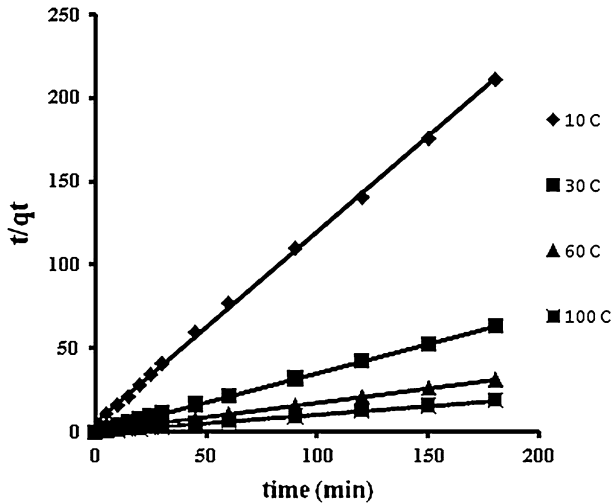


Fig. 9 Pseudo-second order kinetic model of phenol sorption on polyaniline Zr(IV) molybdophosphate Lagergren pseudo-first order [42] and pseudo-second order [43] equations. The pseudo-first order expression is given by Eq. 10:

$$\log (q_e - q_t) = - \left(\frac{K_1}{2.323} \right) \times t + \log q_e \quad (10)$$

Here, q_e is the amount of adsorbate adsorbed per unit weight of adsorbent at equilibrium (mg/g), q_t is the amount of phenol adsorbed per unit weight of adsorbent at any given time t , k_1 is the rate constant for pseudo-first order model. The values of k_1 and q_e (cal) were calculated from slope and intercept of the linear plots of $\log (q_e - q_t)$ versus t at various concentrations.

The pseudo-second order rate expression is used to describe chemisorption involving valency forces through the sharing or exchange of electrons between the adsorbent and adsorbate as covalent forces, and ion exchange [44]. The pseudo-second order adsorption rate equation is given as:

$$\frac{t}{q_t} = \frac{1}{K_2 \times q_e^2} + \frac{1}{q_e} \times t \quad (11)$$

Table 5 Pseudo-first order and pseudo-second order rate constants for adsorption of phenol

Concentration (mg/L)	Pseudo-first order kinetics			Pseudo-second order kinetics				
	K_1 (min^{-1})	q_e (cal) (mg/g)	R^2	q_e (exp) (mg/g)	q_e (cal) (mg/g)	K_2 (g/mg/min)	h (mg/g)	R^2
10	0.063	1.894	0.913	0.851	0.870	0.254	0.193	0.994
30	0.032	0.523	0.948	2.849	2.870	0.228	1.885	0.996
50	0.043	0.676	0.979	5.804	5.830	0.223	7.581	0.998
100	0.020	0.387	0.687	9.600	9.615	0.240	22.271	0.999

Here, h is the initial adsorption rate (mg/g/min), which is given as $h = k_2 \times q_e^2$. k_2 (g/mg²/min) is the adsorption rate constant for the pseudo-second order reaction. The values of k_2 were calculated from the slope of the linear plots of t/q_t versus t at different initial phenol concentrations (Fig. 9).

Table 5 provides data of pseudo-first order rate constants k_1 , pseudo-second order rate constants k_2 , initial adsorption rate (h), the coefficient of determination (R^2), calculated equilibrium adsorption capacity q_e (cal) and experimental equilibrium adsorption capacity q_e (exp). It was found that q_e values calculated from pseudo first order kinetic model q_e (cal) at various initial phenol concentrations differed appreciably from the experimental values q_e (exp) showing that system did not follow pseudo-first order model. In the pseudo-second-order kinetic model, the q_e (cal) were very close to q_e (exp) values at various initial phenol concentrations as compared to pseudo-first-order model. The high values of determination coefficient (R^2) also indicate that the pseudo-second order model is better obeyed by the system.

Conclusions

A novel nanocomposite has been synthesized by the sol–gel method and its adsorption properties have been explored using batch process. The results show that PZMP possessed good adsorption ability for phenol. FTIR, SEM, TEM, XRD analysis demonstrated that the synthetic material is the original design goals. The optimum pH for the adsorption is 4 to 6. Thermodynamic parameters indicate endothermic and spontaneous nature of adsorption. The mean free energy value shows that adsorption is physical in nature. The Langmuir and Freundlich isotherm models are well fitted as indicated by the regression coefficients. The kinetic data proved that pseudo-second order kinetics is applicable model since q_e values calculated from the model are very close to q_e determined experimentally. Hence synthesized PZMP is an effective adsorbent and can be utilized to reduce phenol concentration from aqueous solution prior to its disposal.

Acknowledgments The authors are thankful to the UGC for providing financial support and one of the author thanks to Dean, College of Engineering, Majmaah University for motivation and support. The Research Facilities provided by Department of Chemistry A.M.U Aligarh is gratefully acknowledged.

References

1. Calace N, Nardi E, Petronio BM, Pietroletti M (2002) *Environ Poll* 118:315–319
2. Akbal F, Onar AN (2003) *Environ Mon Assess* 83:202–295
3. Dutta NN, Patil GS, Brothakur S (1992) *Sep Sci Tech* 27:1435–1448
4. Li D, Wu Y, Feng L, Zhang L (2012) *Bioresour Technol* 113:121–126
5. Thu PTT, Dieu HT, Phi HN, Viet NNT, Sung J, Kim VV (2012) *J Porous Mat* 19:295–300
6. Nadavala SK, Boddu VM, Abburi K (2009) *J Hazard Mater* 162:482–489
7. Wang H, Liu W, Yao W, Zhang KE, Zhong J, Chen R (2013) *Appl Surf Sci* 268:179–187
8. Jin L, He D, Wei M (2011) *Chem Eng Tech* 34:1559–1566
9. Jin X, Li Y, Yu C, Ma Y, Yang L, Hu H (2011) *J Hazard Mater* 198:247–256
10. Lin K, Pan J, Chen Y, Cheng R, Xu X (2009) *J Hazard Mater* 161:231–240

11. Soylak M, Elci L, Dogan M (1996) *Trace Elem Electr* 13:130–132
12. Ruiz-Hitzky E, Aranda P, Serratos JM (2004) *Handbook of Layered Materials*. Marcel Dekker, New York
13. Ruiz-Hitzky E, Aranda P, Casal B, Galvan JC (1995) *Adv Mater* 7:180–184
14. Clearfield A (2000) *Solv Extrn Ion Exch* 18:655–678
15. Bushra R, Shahadat M, Raeisssi AS, Nabi SA (2012) *Desalination* 289:1–11
16. Shahadat M, Nabi SA, Bushra R, Raeisssi AS, Umar K, Ansari MO (2012) *RSC Advances* 2:7207–7220
17. Faridbod F, Ganjali MR, Dinarvand R, Norouzi P (2007) *African J Biotechnol* 6:2960–2987
18. Li XG, Ma XL, Huang MR (2009) *Talanta* 78:498–505
19. Lu QF, Huang MR, Li XG (2007) *Chem Eur J* 13:6009–6018
20. www.merck-chemicals.com
21. Laszlo K, Szucs A (2001) *Carbon* 39:1945–1953
22. Li Xin-Guili, Hung MR, Liu R (2005) *React Funct Polym* 2:285–294
23. Rao CNR (1963) *Chemical applications of infrared spectroscopy*. Academic Press, New York
24. Lin CW, Hwang BJ, Lee CR (1999) *Mater Chem Phys* 58:114–120
25. Choudhury A (2009) *Sens Actuat B* 138:318–325
26. Nabi SA, Naushad Mu, Inamuddin (2007) *J Hazard Mater* 142:404–411
27. Chai XL, Zhao YC (2006) *J Hazard Mater* 137:410–417
28. Dabrowski A, Podkoscielny P, Hubicki M, Barczak M (2005) *Chemosphere* 58:1049–1070
29. Langmuir I (1916) *J Am Chem Soc* 38:2221–2295
30. Kalavathy MH, Miranda LR (2010) *Chem Eng J* 158:188–199
31. Dias Flores PE, Lopez Urias F, Terrones M, Rangel-Mandez JR (2009) *J Colloid Interface Sci* 334:124–131
32. Freundlich HMF (1906) *J Phys Chem* 57:385–471
33. Adamson AW, Gast AP (1997) *Physical chemistry of surfaces*, 6th edn. Wiley-Interscience, New York
34. Tabak A, Eren E, Afsin B, Caglar B (2009) *J Hazard Mater* 161:1087–1094
35. Temkin MI, Pyzhev V (1940) *Acta Phys-Chim Sin* 12:327–356
36. Aharoni C, Ungarish M (1977) *J Chem Soc, Faraday Trans* 73:456–464
37. Dubinin MM, Radushkevich LV (1947) *Phys Chem Sec C* 55:331–337
38. Gonzalez JR, Videa JRP, Rodriguez E, Delgado M, Gardea-Torresdey JL (2006) *Biores Techn* 97:178–182
39. Helfferich F (1962) *Ion exchange*. McGraw-Hill, New York 166
40. Liu Y (2009) *J Chem Engg Data* 54:1981–1985
41. IUPAC (1947) *Compendium of chemical terminology*, 2nd edn. Blackwell Science, Oxford, U.K
42. Lagergren S (1898) *About the theory of so called adsorption of soluble substances*. Kung Sven Vetensk Adam Handl 24:1–39
43. Ho YS, McKay G (2000) *Water Res* 29:297–305
44. Ho YS, McKay G (1998) *Process Saf Environ* 6:332–340